CURRENT REARRANGEMENT IN MERGING START-UP OF SPHERICAL TOKAMAK PLASMAS

[1]M. INOMOTO, [1]Y. MAEDA, [2]T. SUZUKI, [2]H. JIN, [2]Y. TOGO, [1]S. CHO, [1]H. UEO, [1]M. OTSUKA, [1]T. KONO, [2]E. SAKURABA, [3]E. KAWAMORI, [4]S. USAMI, [4]R. YANAI

[1]Graduate School of Frontier Sciences, The University of Tokyo, Kashiwa, Japan
[2]Graduate School of Engineering, The University of Tokyo, Bunkyo, Japan
[3]National Cheng Kung University, Tainan, Taiwan
[4]National Institute for Fusion Science, Toki, Japan

Email: inomoto@k.u-tokyo.ac.jp

By utilizing plasma merging technique that provides high power ion heating, it is expected that the operation scenarios of spherical tokamak (ST) fusion reactors will be significantly expanded [1, 2]. For practical application of the merging technique, it is necessary to establish an ion heating scaling law, an appropriate device design for both initial plasma formation and merging of two plasmas along the central axis, and then to realize a smooth transition process to high-beta ST equilibrium while maintaining good confinement performance. In this paper, the plasma current rearrangement mechanism during/after plasma merging was investigated. It was observed that Z-component of the plasma current due to the parallel electric field and that due to the polarization current almost cancel each other out in the reconnection current layer, resulting in the condition that only the toroidal current flows. This polarization current is considered to contribute to the formation of the current profile that confines a finite beta plasma.

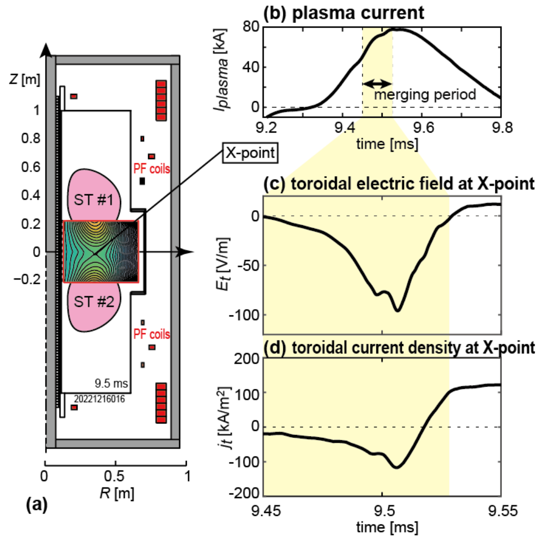

Fig. 1 (a) Schematic cross-sectional view of the UTST device, and waveforms of (b) plasma current, (c) toroidal electric field and (d) toroidal current density at the X-point.

In the UTST device, the formation and merging of initial plasmas are achieved using only the poloidal field (PF) coils located outside the vacuum vessel as shown in Fig. 1(a). The two plasmas generated in the upper and lower formation sections merge via magnetic reconnection at the device equatorial plane of $Z = 0$. The merging process is monitored by a two-dimensional array of pickup coils, Langmuir probes and Rogowski coils. Typical waveforms of total plasma current, toroidal electric field E_t, and toroidal current density j_t observed at the reconnection X-point, are shown in Fig. 1(b-d). The plasma merging occurs just before the current peaks, and the period with strong toroidal electric field E_t is about 0.03 ms. Since the plasma current of the ST flows in the positive toroidal direction, a thin negative current layer is formed between the two ST plasmas during merging. The time evolution of the radial profile of the toroidal current density profile on $Z = 0$ plane is shown in Fig. 2. A negative toroidal current is observed in the early stage of merging (t = 9.49 ms), but a positive current gradually grows in the radially inner region, eventually resulting in a hollow current profile of a merged ST equilibrium (t = 9.52 ms). To understand such changes in the current profile, it is necessary to clarify the electric field structure in the reconnection current layer and the downstream region.

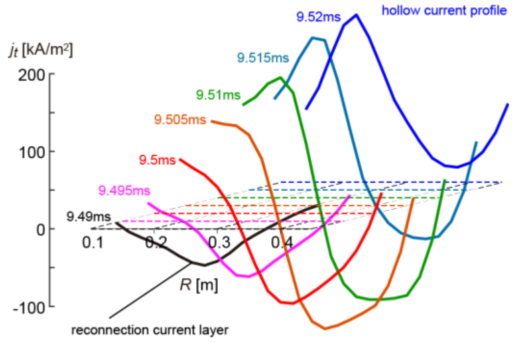

Fig. 2 Time evolution of the radial profile of the toroidal current density on Z = 0 plane.

Unlike magnetic reconnection that occurs between antiparallel magnetic fields, reconnection in ST merging includes a guide magnetic field (toroidal magnetic field) that is perpendicular to

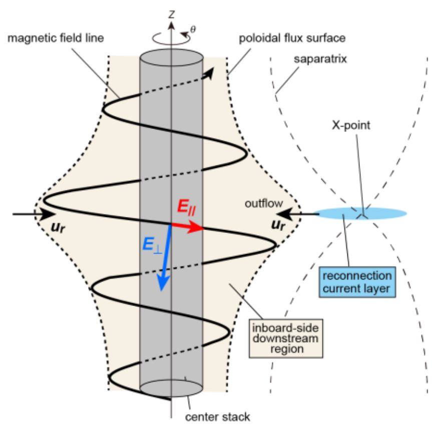

Fig. 3 Schematic view of electric field decomposition in the downstream region.

the reconnecting magnetic fields, which causes the induced toroidal electric field to have a component parallel to the magnetic field. As a result, a quadrupole structure of electrostatic potential is formed spontaneously, and the electrostatic field has a significant effect on reconnection physics as well as the plasma behavior in the downstream region [3]. Both the inductive and electrostatic fields are measured on the reconnection plane ($Z = 0$) by using pickup coil array and Langmuir probe array and decomposed into components parallel and perpendicular to the magnetic field as shown in Fig. 3. Since $|B_t| \gg |B_z|$ and $B_r \simeq 0$ on $Z = 0$ plane, the conditions of $|E_{//,t}| \gg |E_{//,z}|$ and $|E_{\perp,z}| \gg |E_{\perp,t}|$ hold.

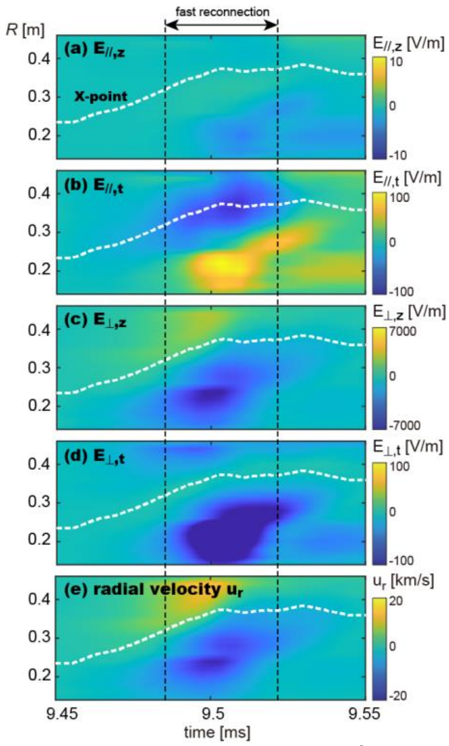

Fig. 4 Spatiotemporal evolutions of (a,b) Z- and toroidal components of the electric field parallel to the magnetic field and (c, d) those of the electric field perpendicular to the magnetic field measured on Z = 0. (e) Radial outflow velocity calculated by $E \times B$ drift.

Figure 4 (a-d) show the evolution of Z- and toroidal components of the electric field parallel and perpendicular to the magnetic field. Note that $\boldsymbol{E}_{//}$ exists not only near the X-point indicated by white dashed line ($R{\sim}0.35$ m in (b)) but in the inboard-side downstream region ($R{\sim}0.2$ m in (b)) but although its sign is reversed. This fact indicates that the steady MHD condition of $\boldsymbol{E}_{//} \simeq 0$ is broken in the downstream region due to the excessive charge separation [4], which also enhances $\boldsymbol{E}_{\perp}$ in the downstream region ($R{\sim}0.2$ m in (c, d)). The evolution of radial outflow velocity u_r on the midplane ($Z = 0$) calculated from the $\boldsymbol{E}_{\perp} \times \boldsymbol{B}$ drift velocity is shown in Fig. 4(e). As expected from the reconnection geometry, the radial flow originates from the X-point.

Based on the observed transient electric fields, electrical currents flowing in the reconnection current layer and in the reconnection downstream region are evaluated based on the parallel current $\boldsymbol{j}_{//} = \boldsymbol{E}_{//}/\eta_{\mathrm{eff}}$ and the polarization current [5] $\boldsymbol{j}_{\perp} = (\rho/B^2)d\boldsymbol{E}_{\perp}/dt$, where η_{eff} is the effective resistivity in the reconnection region and ρ is the mass density. Regarding the toroidal component, the contribution of the polarization current (solid lines) is very small and most of the current is carried by the parallel current (dashed lines) as shown in Fig. 5(a). Negative toroidal current flows at the X-point and in the reconnection current layer (highlighted in light blue) where the stretched magnetic field lines contract to accelerate plasma outflow, while positive current flows in the inboard-side downstream region (highlighted in light yellow) where magnetic flux accumulates just in front of the center stack.

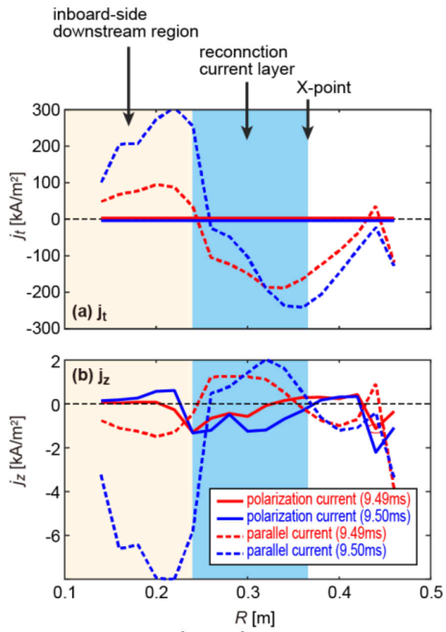

Fig. 5 Radial profiles of (a) toroidal and (b) Z-components of the current density evaluated from the parallel current and the polarization current.

Regarding the Z-component, on the other hand, a non-negligible amount of the polarization current flows in the reconnection current layer as shown in Fig. 5(b). The polarization current almost cancels out the Z-component of the parallel current, and as a result, only the toroidal current exists in the reconnection current layer. In other words, the electrical current flowing in the reconnection current layer where the magnetic field lines have concave shapes does not affect the charge separation in Z-direction that maintains the macroscopic plasma motion. Then in the downstream region where the magnetic flux accumulates, parallel current is driven in the negative Z-direction by the parallel electric field due to the excess charge separation, forming a convex magnetic field line shape of the merged ST. Since the polarization current flows in a direction that reduces the parallel current, it is suggested that the paramagnetism of ST is suppressed and a transition to a high-beta equilibrium occurs.

These experimental results suggest that both the inductive electric field and the electrostatic field play an essential role not only in maintaining the macroscopic plasma flow associated with plasma merging, but also in forming the current profile that maintains the finite beta ST equilibrium after merging.

[1] ONO, Y., et al., Nucl. Fusion **64** (2024) 086020.
[2] MCNAMARA, S.A.M., et al. Nucl. Fusion **63** (2023) 054002.
[3] INOMOTO, M., et al., Nucl. Fusion **61** (2021) 116069.
[4] INOMOTO, M., et al., Nucl. Fusion **64** (2024) 086060.
[5] JI, H., et al., Space Science Reviews (2023) 219:76.